

## Numerical analysis of supersonic pulse jets

by

Ryuji ISHII, Yoshikuni UMEDA, Graduate School, Kyoto University

and

Masatoshi YUHI, Kanazawa University

## ABSTRACT

Unsteady circular jets are treated numerically. The time evolution of circular pulse jets is investigated systematically in a wide range of jet strength. Focus is placed on the jet evolution, in particular, the formation process of Mach disks in the middle stage and of shock-cell structures in the later stage. It is shown that unsteady Mach disks are realized at least temporarily for all sonic underexpanded jets, but they decay with time for weak jets. The vortex ring produced near the nozzle lip plays an important role in the formation of the shock-cell structure. Especially interactions between the vortex ring and the Mach disk connected with a strong second shock affect remarkably the construction process of the first shock-cell. A few types of different construction processes of the first cell structure are found. It is also made clear that the Kelvin-Helmholtz instability along slip surfaces originating from the triple point at the outer edge of the Mach disk is responsible for the generation of large second vortices which enroll the first vortex. This results in strong mixing of the jetting gas and the gas around the jet.

## 1. Introduction

Supersonic jets have been used in many research fields and also realized in many practical applications. Laminar supersonic jets are used in the aerodynamic levitation flow reactors. In kraft recovery boilers, supersonic jets are applied as sootblowers to remove the fireside deposit. They are used for gas atomization of melt metal to produce small metal powders and also for oxygen-fuel flame spraying. At the lift-off of a rocket, unsteady supersonic jets are exhausted from nozzles just after the ignition. At the operation of an air bag in a car, an unsteady supersonic jet is applied. Furthermore, recently, it has been recognized that pulsed supersonic jets provide effective means to control the chemical energy release in variety of combustion system - as utilized in advanced concepts

for internal combustion engines.<sup>1</sup>

In the present paper, unsteady circular jets are treated numerically. Gas (air) is accelerated by a shock in a shock tube with a constant circular cross section and exhausted from the open end into a test chamber. So the jet strength is controlled by one parameter  $p_4/p_1$ , where  $p_1$  and  $p_4$  are initial gas pressures at the low pressure chamber and a high pressure one, respectively. The pressure ratios were chosen in the range from 2.0 to 50. The basic flow characteristics of the unsteady jet are investigated systematically. Focus is placed on the jet evolution in the second and third stages. The Kelvin-Helmholtz instability and the generation of the second vortices are investigated in detail in relation to the formation process of a Mach disk. It will be made

clear that the Kelvin-Helmholtz instability along the slip surface plays a very important role in the jet instability. The numerical results are compared with the experiments and good agreement is obtained between them.

## 2. Numerical Simulation

The numerical simulations were performed on a supercomputer Fujitsu VP-2600 at the Data Processing Center of Kyoto University. The Euler equations for an axially symmetric flow were solved by a finite-difference TVD scheme proposed by Chakravarthy and Osher.<sup>2</sup> The mesh number is  $600 \times 400$ . On the outer boundary and the downstream boundary, the ambient gas condition is applied;  $(p, \rho, u, v) = (p_1, \rho_1, 0, 0)$ , where  $\rho$  is the gas density,  $u$  the axial velocity and  $v$  the radial velocity of the gas flow. On the solid walls and the jet axis, the symmetric condition is applied. On the upstream boundary inside the shock tube, the shock condition  $(p, \rho, u, v) = (p_2, \rho_2, u_2, 0)$  is applied, where the quantities denoted by the subscript 2 are obtained through the Rankine-Hugoniot relations for a specified shock Mach number  $M$ .

In the numerical simulation, the effect of the boundary conditions are responsible for serious artificial or unrealistic phenomena. This is because in the present case, the outer and the downstream boundaries do not correspond to the actual boundaries. Empirically it is well known that the downstream boundary can affect the numerical results relatively remarkably. Numerically it was confirmed that the effect of the outer boundary does not affect appreciably the jet evolution, if the axial length is taken more than 5 times the size of the duct radius. So the total radius of the computational domain is taken to be 10, where the nondimensional duct radius  $L_s = \frac{1}{2}D_s$  is taken to be unity.

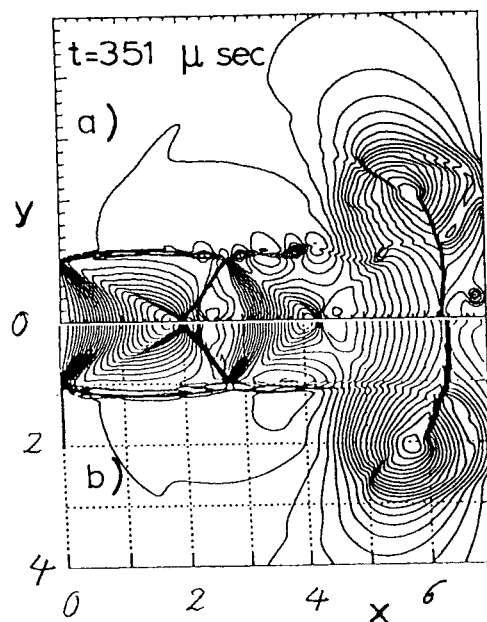


Fig.1 Effect of mesh size.

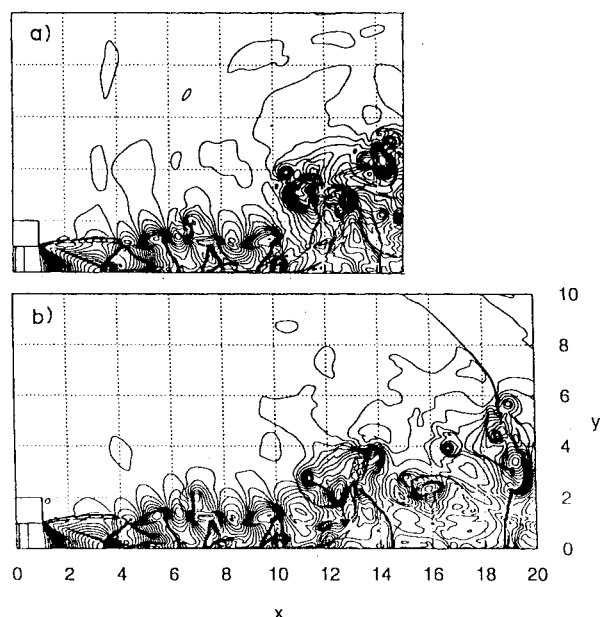


Fig.2 Effect of downstream boundary.

Here we check first the effect of the downstream boundary. Fig. 1 shows the density contours of a jet for  $p_4/p_1 = 12.0$  at  $1140 \mu \text{ sec}$ , where  $x$  and  $y$  are the axial and radial coordinates, respectively, nondimensionalized by the duct radius  $\frac{1}{2}D_s = 1 \text{ cm}$  ( $D_s = 2 \text{ cm}$ ). The nondimensional mesh sizes ( $\Delta x, \Delta y$ ) are set as  $(0.05, 0.05)$ . Only one difference between the jets a) and b) is the length of the downstream boundary from the upstream one. It was taken to be 15 in the case a) and 20 in the case b). Obviously, both jet

structures are almost the same with each other for  $0 \leq x \leq 10$  except for some weak pressure waves surrounding the jets. In the present study, we can visualize and then investigate the jets only in the circular region with a radius 4 (cm) whose center is located at about  $(x, y) = (4, 0)$ . This suggests that the 15 times of the duct radius is quite sufficient as the axial length of the computational domain to investigate reasonably the jet evolution up to time 1000  $\mu\text{sec}$  in the numerical simulation.

We will also check the effects of the mesh size on the numerical results. Here we note that a square mesh was used ( $\Delta x = \Delta y$ ) throughout the present paper. It is generally well known that the numerical results depend on the mesh size. So it is crucially important to see what kinds of phenomena we can predict by the numerical simulation. Figs. 2-a) and 2-b) show the density contours of a jet for the pressure ratio  $p_4/p_1 = 8.7$  at 351  $\mu\text{sec}$ . As we can see, the both results agree quite well with each other. Only one difference between the computational conditions is the mesh size  $\Delta x (= \Delta y)$ . In the former case,  $\Delta x$  is set at 0.025 and it is set at 0.05 in the latter case. From these results, we can expect that the strong phenomena such as jet boundary, expansion waves, shock wave and strong vortical structure can be well predicted in the unsteady pulse jets. Only the Kelvin-Helmholtz role-up and the resultant fluctuations depend appreciably on the mesh size. In what follows, the mesh size  $\Delta x = \Delta y = 0.025$  is taken as a reference mesh size. The present TVD-scheme can solve the one-dimensional shock tube problem with 99.9 % accuracy. A normal shock can be captured with 4 or 5 meshes.

### 3. Numerical results

It is well-known that the TVD scheme is very effective and powerful to simulate

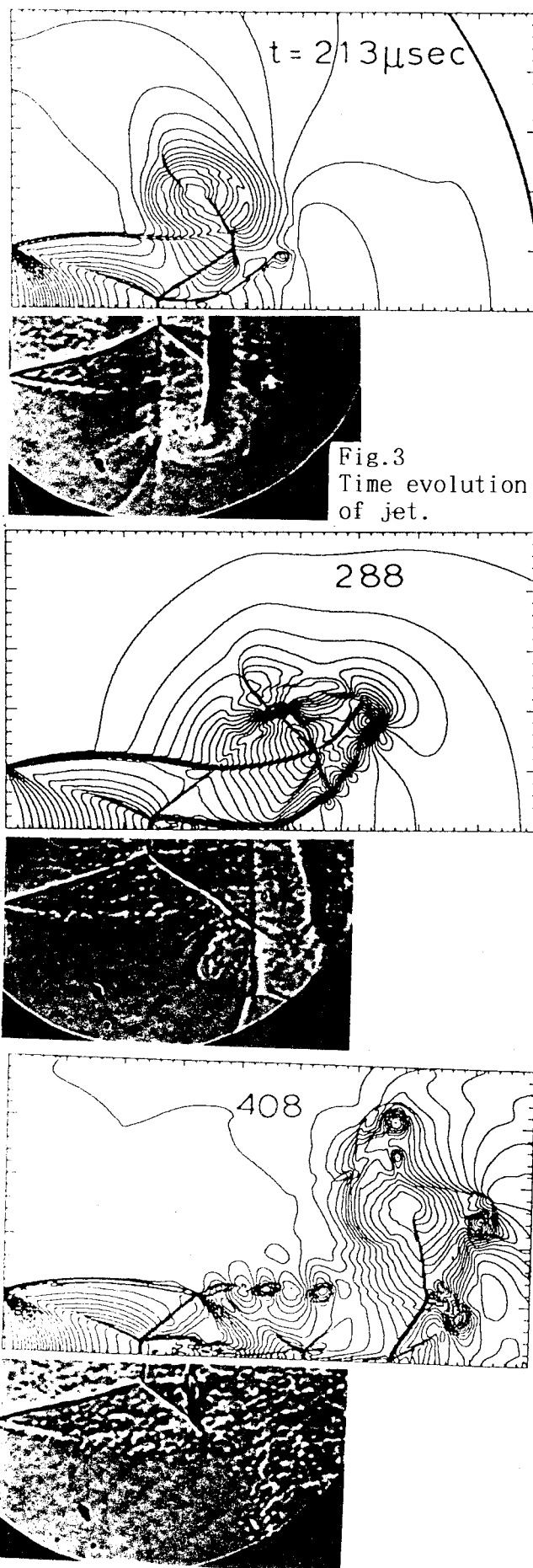


Fig.3  
Time evolution  
of jet.

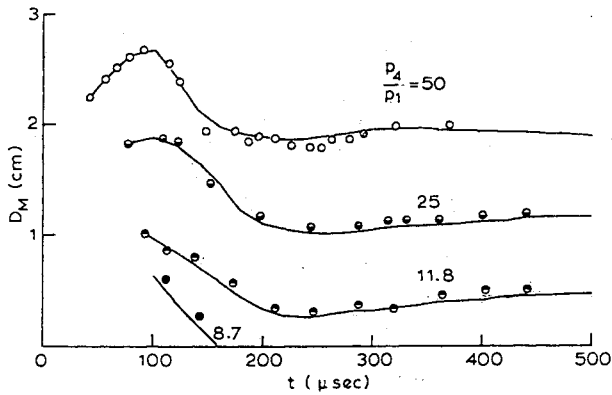


Fig. 4 Diameter Mach disk diameter.

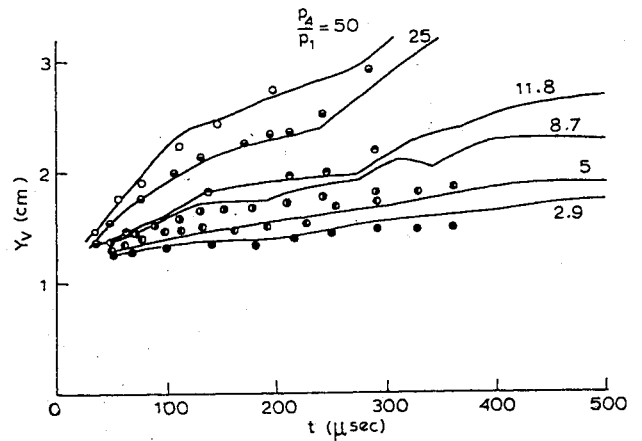


Fig. 6 Radial distance of first vortex.

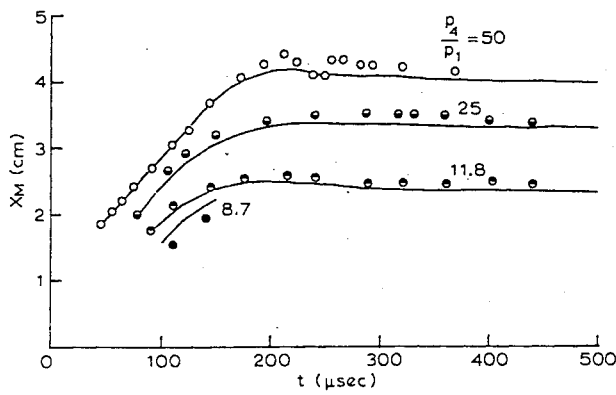


Fig. 5 Axial distance of Mach disk.

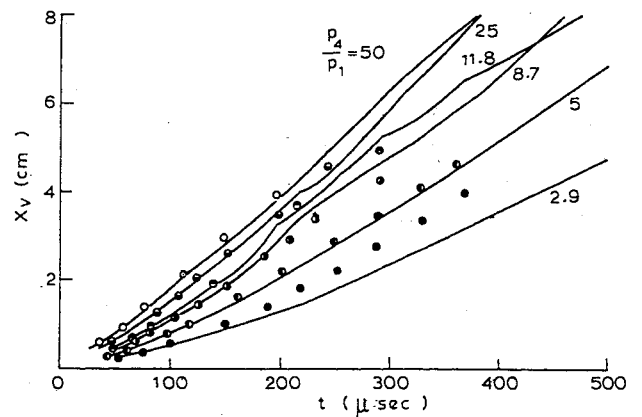


Fig. 7 Axial distance of first vortex.

flow fields with shock discontinuities. This scheme can also be applied directly to the Navier-Stokes equations. But when the Navier-Stokes equations are used, appropriate mesh refinement is inevitable in local flow regions where the viscous effect is important. In the present study, the jet evolution is essentially unsteady and then it is almost impossible to guarantee a sufficient number of meshes in these local moving flow regions due to lack of capacity of the computer resources.

A sample of the jet evolution is shown in Fig. 3 for  $p_4/p_1 = 11.8$ . The solid lines and circles denote the numerical and experimental results, respectively. The center of the first vortex is clearly seen in both the numerical and experimental

jets at  $t = 213 \mu\text{sec}$  and  $288 \mu\text{sec}$ . At  $t = 231 \mu\text{sec}$ , the first shock cell is elongated by the reflected shock connected with the second shock. At  $t = 408 \mu\text{sec}$ , the first shock cell shrinks by a few percent. The jets have a few strong second vortices around the first vortex. They are convected around the first vortex faster and even reach upstream side of it. The shocks and slip lines are simulated very well.

We will investigate more systematically the characteristics of unsteady jets. For the time evolution of the diameter  $D_M$  and the axial distance  $X_M$  of the Mach disks are shown in Figs. 4 and 5, respectively. Obviously good agreement between the numerical and experimental results is obtained. The diameter  $D_M$  increases with

time after its formation for the strong jets ( $p_4/p_1 = 25$  and  $50$ ), decreases to a minimum value and then tends to increase very gradually to some quasi-steady value. In the jet for  $p_4/p_1 = 11.8$ ,  $D_M$  decreases after the formation and becomes minimum at about  $t = 250 \mu\text{sec}$  and then begin to increase. It is interesting that the jets for  $p_4/p_1 = 11.8, 25$  and  $50$  take their minimum diameters at nearly the same time  $t \sim 250 \mu\text{sec}$ . It is also interesting that the jet for  $p_4/p_1 = 8.7$  has an unsteady Mach disk temporarily but does not construct any quasi-steady Mach disk. The axial distance  $X_M$  experiences a weak overshooting at  $t = 200 \sim 300 \mu\text{sec}$  and then tends to decrease slightly to some quasi-steady value.

Next the motions of the first vortices ( $X_v, Y_v$ ) are plotted in Figs. 6 and 7, respectively, where ( $X_v, Y_v$ ) denote visual centers of the first vortex. The identification of the vortical center is very difficult experimentally. Agreement between the numerical and experimental results is rather poor in a later stage. This trend is prominent for the weakest and the strongest jets ( $p_4/p_1 = 2.9$  and  $50$ ), respectively. In the former jet, any shock wave is not formed behind the first shock and then the jet evolution will be viscosity dominant. In the latter jet, very strong second vortices are generated and their motion will also be affected appreciably by the gas viscosity.

#### 4. Conclusion

Unsteady circular jets were investigated

numerically in a wide range of the jet strength. After a sudden gas outflow, there are several stages in the subsequent time evolution of a sonic or supersonic underexpanded jet. The first stage is the diffraction of the first shock at the end corner. The second stage is the formation of an unsteady Mach disk or a normal shock. It was shown that the formation process of the Mach disk is not unique. Even in the jet which does not have a quasi-steady Mach disk, an unsteady Mach disk can be realized at least temporarily. The third stage is the formation of the first shock-cell structure. This stage is strongly affected by the presence of the first vortex and the Mach disk. As soon as the connection between the second shock and the reflected shock is interrupted, the shock-cell length becomes maximum and thereafter it tends to shrink to a certain asymptotic size. The jet with a strong Mach disk is very unstable and rapidly break up. The jet tip is folded back on itself and is entrained into the first vortex ring and soon later evolves to a fully-developed turbulent flow. It has been confirmed that the numerical results obtained by a TVD scheme for the Euler equations can predict successfully the construction process of the shock-cell. Especially the shock-cell with a Mach disk is remarkably well simulated quantitatively as well as qualitatively.

#### References

- 1) A.L. Kuhl, H. Reinhenbach, P. Neuwald, R. E. Ferguson, and A. K. Oppenheim, Fluid Mechanics of a Planner Exothermic Jet. JSME ICFE-97, pp.955-959 (1997).
- 2) S.R. Chakravarthy, and S. Osher, A New Class of High Accuracy TVD Schemes for Hyperbolic Conservation Laws. AIAA Paper 85-0363 (1985).

